ePublishing

HNPS Advances in Nuclear Physics

Vol 22 (2014)

HNPS2014

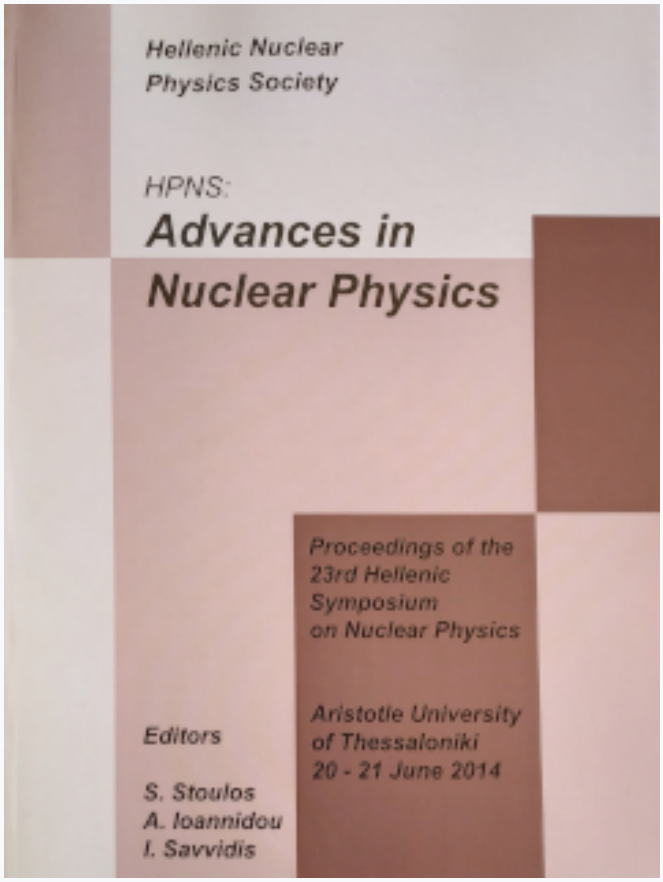

The benchmarking procedure: Implementation in the case of proton backscattering

V. Paneta, J. Colaux, A. Gurbich, C. Jeynes, M. Kokkoris, A. Lagoyannis

doi: 10.12681/hnps.1931

To cite this article:

Paneta, V., Colaux, J., Gurbich, A., Jeynes, C., Kokkoris, M., & Lagoyannis, A. (2019). The benchmarking procedure: Implementation in the case of proton backscattering. *HNPS Advances in Nuclear Physics*, *22*, 56–66. https://doi.org/10.12681/hnps.1931

https://epublishing.ekt.gr | **e-Publisher:** EKT | **Downloaded at:** 22/01/2026 02:47:00

The benchmarking procedure: Implementation in the case of proton backscattering

V. Paneta[1,2], J. Colaux[3], A. Gurbich[3], C. Jeynes[3], M. Kokkoris[2], A. Lagoyannis[1]

[1] *Tandem Accelerator Laboratory, Institute of Nuclear Physics, N.C.S.R. "Demokritos", 15310 Athens, Greece*
[2] *Department of Physics, National Technical University of Athens, 15780 Athens, Greece*
[3] *University of Surrey Ion Beam Centre, Guildford GU2 7XH, England, United Kingdom*

Abstract
The benchmarking procedure in IBA regards the validation of charged-particle differential cross-section data via the acquisition of EBS spectra from uniform thick target of known composition followed by their detailed simulation. In the present work such benchmarking measurements have been performed for the elastic scattering of protons on ^{23}Na, ^{31}P and ^{nat}S in the energy range of 1–3.5 MeV in steps of 250 keV at three backward angles, at 120.6°, 148.8° and 173.5° in order to validate the corresponding existing evaluated cross-section datasets from SigmaCalc and to facilitate their extension at higher energies. The measurements were performed using the 2 MV Tandetron Accelerator of the Ion Beam Center of the University of Surrey. The EBS spectra acquired were compared with simulated ones using the DataFurnace code, along with an a posteriori treatment of the surface roughness. All the experimental parameters were thoroughly investigated and the results obtained and the discrepancies found are discussed and analyzed. Moreover, the benchmarking procedure in complicated cases, such as the ^{nat}B(p,p) studied at NCSR "Demokritos", where background contributions exist, is also discussed.

1. Introduction

Ion Beam Analysis (IBA) techniques, such as Elastic Backscattering Spectroscopy (EBS) and Nuclear Reaction Analysis (NRA), are widely used in material studies to quantify the concentration of light natural elements and isotopes in complex samples while simultaneously providing depth profiling data. The accurate application of these analytical techniques critically depends on the accuracy of the cross sections of the reactions involved. The evaluated cross-section data, available through the online calculator SigmaCalc [1], are the most reliable data to be used in analytical studies, since they involve a critical assessment of the available experimental data, which are often scarce and/or discrepant, followed by a proper tuning of the corresponding nuclear model parameters [2]. However, most of the evaluated datasets are still not adequately validated. A carefully designed benchmarking experimental procedure, which regards the actual validation of differential cross-section data via the acquisition of thick target spectra followed by their simulation, is thus mandatory. Benchmarking can also provide feedback for the adjustment of the parameters of the nuclear model used in the evaluation process, and can help in assigning realistic uncertainties to the cross sections. Moreover in the absence of evaluated cross sections, it can indicate recommended experimental datasets. In the past, benchmarking results have usually been reported, related to the validity of specific experimentally determined differential cross-section datasets [e.g. 3-5]. However, such measurements have never been performed in a systematic and consistent way, taking into account all the fine steps and details of the benchmarking process.

The present work contributes in this field exactly by developing a methodology for this process, concerning the detailed investigation of all the involved parameters, thus

defining the necessary steps for the benchmarking process, described in the beginning of this chapter following a brief description of the general methodology and concept. Within this framework, benchmarking measurements were performed for the validation of important cross sections relevant to IBA, concerning the evaluated data for the proton elastic scattering on ^{23}Na, ^{31}P and ^{nat}S in the energy range of 1–3.5 MeV, facilitating also their extension to higher energies. A different approach is also proposed, for studying the cases, where there is background contribution of alpha particles (originating from (p,α) reactions) inhibiting the benchmarking process of the proton elastic backscattering, as investigated for the benchmarking study of the ^{nat}B(p,p) reaction. Boron is widely used not only in the semiconductor industry as dopant/impurity in silicon and germanium substrates, but also in nuclear technology as the main reactor moderator. The quantification and depth profile of boron in all applications is thus critical but unfortunately the existing cross section data for the implementation of the IBA techniques in the field is rather discouraging, due to the fact that there existing significant discrepancies.

2. Experimental setup

The measurements for the benchmarking on the proton backscattering on ^{23}Na, ^{31}P and ^{nat}S were performed in one comprehensive run using the 2 MV GVM Tandetron Accelerator at the Ion Beam Centre at the University of Surrey, England. Spectra of elastically backscattered protons from ^{23}Na, ^{31}P and ^{nat}S, using uniform thick targets were systematically measured in the energy range of 1-3.5 MeV, in steps of 250 keV, at 120.6°, 148.8° and 173.5° with an uncertainty of 0.1°. The scattering angles were measured directly using a beam-line laser and the six-axis goniometer. The goniometer also allowed for the correct positioning of the targets along the z-axis according to their thickness (1-5 mm). The detection system consisted of three Silicon Surface Barrier (SSB) detectors (thickness of 100μm), placed at the corresponding angles, along with the standard electronics for spectroscopy. The thick target spectra from the three detectors were simultaneously recorded at each energy point. The detectors were set at a distance of ~14, 12 and 19 cm from the target, with orthogonal slits having a width of about 2, 2 and 5 mm in front of them, in order to reduce the effective angular uncertainty to ~1°, 1.4° and 2.3° respectively. The proton beam spot was focused to ~1 mm in diameter, while the beam current was kept lower than 20 nA during all measurements, in order to minimize the pileup effects. The targets used were high-purity (>99.99%), highly pressurized tablets of NaBr and MoS_2 in the case of ^{23}Na and ^{nat}S, and a polished crystalline GaP wafer in the case of ^{31}P. A thin layer of gold (of ~$50x10^{15}$ at/cm^2) was evaporated on top of all targets in order to protect them from corrosion and for normalization purposes. The targets were mounted all together on the six-axis goniometer allowing us to avoid channeling effects by tilting the sample and automatically switch from one target to another for each energy step.

The measurements for the benchmarking investigation of the ^{nat}B(p,p) reaction were performed using the 5.5 MV Tandem accelerator located at the Tandem accelerator laboratory of the Institute of Nuclear and Particle Physics of the National Center for Scientific Research "Demokritos" in Athens, Greece. Protons in the energy range of 1500-3300 keV were led to a large scattering chamber (R~40cm) and were backscattered by a ^{nat}B pellet with a thin layer of gold on top and were detected from SSB detectors at 120° and 170° at a distance of ~10 cm, both by using standard NIM electronics and by implementing the ΔE/E technique with the use of event by event acquisition (CAMAC). A ΔE/E telescope consists of two SSB detectors in a row, that is of a very thin transmission one (ΔE) first, in which the detected particles do not deposit their full energy and a thick one (E) exactly behind it, in which they finally stop. The thin detectors used were of 22 and 6 μm in thickness, respectively, while all the thick ones were of 1000μm. The beam spot size was ~2mm in diameter, while the current on the target did not exceed ~5nA during all measurements.

3. Benchmarking steps

The followed procedure of benchmarking is based on the comparison between the acquired thick target spectra and the corresponding simulation of the spectra. The scope of this process is to perform simulations under the same conditions with those of the experiment and then after accurately determining all the parameters involved, affecting the obtained spectra, any possible discrepancies between the simulations and the real experimental spectra can be attributed exclusively to the differential cross-section data used in the simulations (over a restricted energy range, as discussed in the following section).

Benchmarking is therefore an experimental procedure that needs to be very carefully designed. A thick target spectrum is essentially a convolution of the stopping power and the straggling function in the material, the resolution of the detector and the corresponding cross section, but several other parameters are also important for accurate simulations. These include the calibration of the accelerator energy and the ADC, the determination of the accumulated charge in the target and the treatment of possible background counts and/or pile-up effects. Special attention should also be drawn to the proper selection of the thick target used in benchmarking, in terms of its element composition and structure, for several reasons. These mainly concern the background contribution, the charge/solid angle normalization, the plural scattering and the effect of surface/interlayer roughness or channeling. Each of these parameters affects the obtained spectra in a different way, but all of them need to be carefully treated for a proper and accurate validation procedure. In addition to the above, the code used for the simulation should be capable of taking into account any possible fine structure of the corresponding differential cross section (sharp narrow resonances).

For the present benchmarking measurements, all the mentioned parameters were treated in the most detailed possible way, as described in the following paragraphs, while the SIMNRA code [6] and the DataFurnace code [7], which is capable of taking into account the cross-section fine structure and self-consistently fitting multiple spectra, were used for the simulations. The simulated spectra were along these lines produced taking into account a very small energy step for the incoming and outgoing particles, the effect of multiple scattering, the beam ripple, ZBL stopping power data [8], and Chu and Yang's straggling model [9,10] as implemented in the codes used. It should be noted here that for the moment all popular analytical codes do not take the uncertainties in the experimental differential cross-section datasets into account, while the assessment of the uncertainties in the evaluated datasets has been the subject of recent studies [11,12].

3.1 Energy calibration of the GVM accelerator

The final energy of the protons was determined by calibrating the accelerator (GVM) with the use of three narrow resonances, namely the (991.9±0.1) keV one of the $^{27}Al(p,\gamma)^{28}Si$ reaction (Γ=110 eV) [13], the (1747.6±0.9) keV of the $^{13}C(p,\gamma)^{14}N$ reaction (Γ=122 eV) [14] and the (3379±1) keV of the $^{32}S(p,p\gamma)^{32}S$ reaction (Γ=700 eV) [15] using a 10% HPGe detector. The linearity of the energy with respect to accelerating voltage, as shown in Figure 1, was found to be excellent over the whole energy range studied. The uncertainty of the proton energy was calculated to be less than 0.1%.

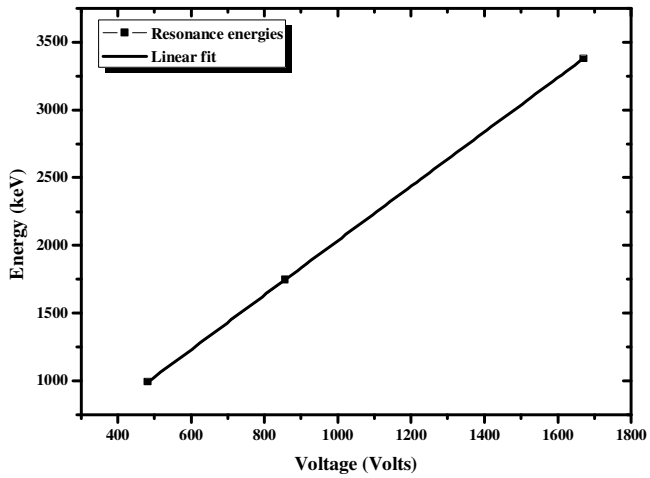

Figure 1. GVM Tandetron accelerator calibration using the three narrow resonances (see text). The error bars are not visible due to the adopted scale.

3.2 Detector resolution and ADC calibration

The simulation of the backscattered protons from the polished GaP target at all three angles studied, compared to the corresponding experimental spectra acquired, enabled simultaneously the calibration of the ADC (Au peak) and the determination of the resolution of all the detectors.

3.3 Stopping power, straggling and plural scattering

The models, which are considered to be the most accurate ones, were used in the DataFurnace code for the simulations. These are the model of Ziegler–Biersack–Littmark [8] for the proton stopping power and the one of Chu & Yang [9,10] for the straggling function. The effect though, of these two parameters, as well as the effect of plural scattering, especially when a heavy element is present in the target, were investigated in the present study by comparing the spectra obtained at close energies (i.e. at resonances and then, in small energy steps above the resonances) and using different stopping power compilations. It was found that the effect of those three parameters could not be simulated in a satisfactory way at lower energies (deeper in the targets), as it can be observed in Figure 2, for the plural scattering effect. Although each of these parameters has a different dependence on depth, all of them are more pronounced, with decreasing energy of the incoming particles. In order to diminish such problems in the simulations, the analysis was limited relatively close to the surface leaving a narrow window of opportunity for the validation of the cross-section data. The energy step for all the benchmarking runs was thus small, not larger than 250 keV, over the whole energy range studied.

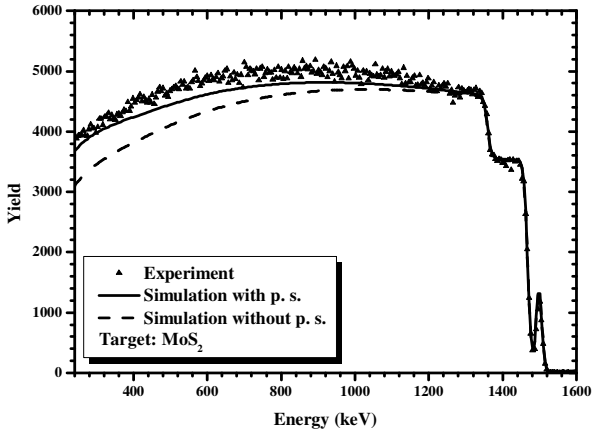

Figure 2. Thick target spectrum (MoS_2) simulated with and without plural scattering at 1531 keV at 148.8°, along with the corresponding experimental spectrum.

3.4 Roughness of the targets

The roughness of the NaBr and MoS_2 pellets used in the present study was treated *a posteriori* using an algorithm based on the mathematical model developed by Molodtsov *et al.* [16]. To take into account the possible secondary crossings of protons in the asperities of the target surface, according to the model, the uncorrected simulated spectrum $Y_0(E)$ is convoluted with a parameterization function f(x), which depends on two free parameters, namely the sharpness p of the asperities and σ, a random height, chosen from a Gaussian distribution of variance σ^2. These parameters were determined using the MINUIT code for χ^2 minimization [17]. As shown in Figure 3, the surface roughness can significantly affect the shape of the spectra and thus, it is very important to treat it carefully when present.

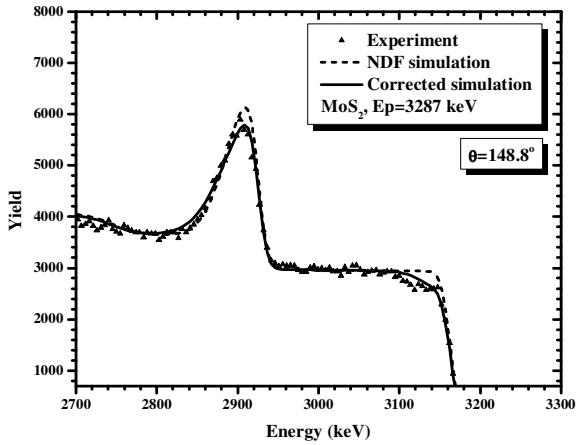

Figure 3. Typical experimental and simulated thick target spectra (MoS_2) along with the corresponding simulation, *a posteriori* corrected for the effect of surface roughness.

4. Assessment of the uncertainty factors

The assessment of the uncertainties of all the parameters involved in the simulating and validating steps is very important for the benchmarking procedure. The obtained simulated yield is directly related to the stopping power systematics. The effect though of different stopping power compilations (e.g. ZBL and Andersen-Ziegler [18]) in the integrated yield of ~40-50 channels (corresponding to 250 keV from the surface) which were used in the validation procedure was always less than 1%. The pulse height defect, related to the energy loss in the dead layer of the detector, has also a negligible effect on the analysis for the proton energy range studied and the ADC width (keV/channel) used.
The important uncertainty factors in the present work are thus related to the counting statistics and the accurate determination of the accumulated charge Q multiplied by the solid angle Ω subtended by a detector (QΩ factor). The effect of these parameters is strongly target dependent. Whenever the target consists of a compound with a high-Z element, on which the elastic cross section does not deviate from the Rutherford formula, the uncertainty in the determination of the QΩ factor is minimized, while the corresponding uncertainty in the statistics is maximized, because one has to subtract the large Rutherford signal of the high-Z element from the total experimental one, in order to validate the cross section for the light element. In the present work, in order to minimize the effect of the QΩ factor uncertainty at high proton energies, where possible deviations from the Rutherford formula could in principle exist for Ga and Br, all data were normalized relative to the Rutherford backscattering on Au. The thickness of the deposited thin Au layers was calculated for each target, by fitting the simulated spectra at several low beam energies (namely at 1531, 1782 and 2033 keV) and detector angles, where proton elastic backscattering on Br, Mo and Ga follows the Rutherford formula and by taking the average value. This procedure yielded an estimated uncertainty of ~3% in all cases, and this was in fact the dominant uncertainty in the validation procedure, except for the case of the NaBr target and the complicated case of ^{nat}B(p,p), which are described in the following section. On the other hand, at lower proton beam energies the uncertainty in the determination of the QΩ factor was minimized, since it was obtained directly from the Br, Mo and Ga signal, following the roughness correction and the dominant uncertainty was thus the statistical error in the experimental yield. In all cases, however, with the exception of ^{23}Na(p,p) and ^{nat}B(p,p), the total combined uncertainty in the present work, including all statistical errors, did not exceed 4% (±1σ).

5. Results and Discussion

Concerning the **^{nat}S(p,p)** reaction, for which the evaluated data go up to 3.5 MeV, typical benchmarking results of the present work, using a MoS_2 pellet with a thin layer of gold on top as target are shown in Figures 4. It is shown that the simulated spectra, using the evaluated cross sections reproduce the experimental ones in an excellent way (within 1-8%) for all the backward angles studied, up to 3287 keV, which was the last benchmark point, where the simulation and the experiment perfectly agree. Cross sections for all intermediate backward detection angles, typically used for EBS measurements, are thereby also validated. In Figure 4c however, it is seen that using the evaluated results from SigmaCalc 1.6 for the ^{nat}S(p,p) backscattering, there are discrepancies between the experiment and the simulation around 3.5 MeV. Following the benchmarking results of the present work, the evaluation was revised (SigmaCalc 2.0) [1], as seen in Figure 4d, leading to a very good reproduction of the experimental spectra, as illustrated in Figure 4c.

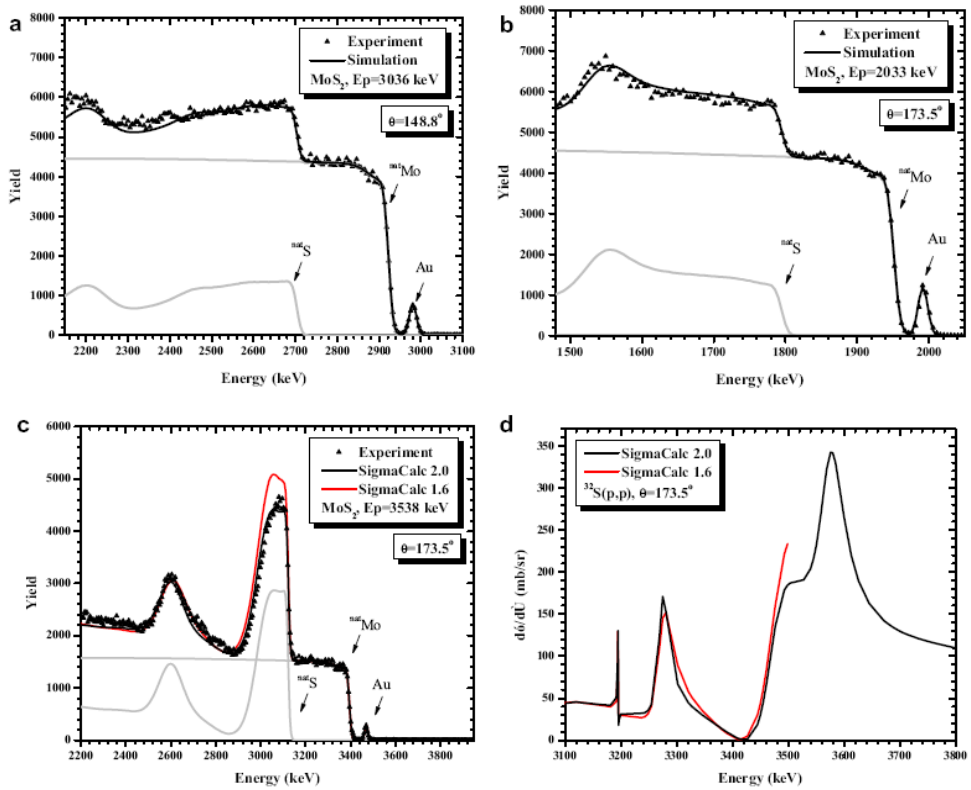

Figures 4. (a–c) Benchmarking results for ^{nat}S(p,p) using the corresponding evaluated cross-section datasets for the simulations at different beam energies and detection angles. (d) Comparison between the two versions of SigmaCalc.

The obtained results for the benchmarking on the proton backscattering on ^{nat}S can be demonstrated online in SigmaCalc website [1]. There exists a full database with all the relevant acquired thick target spectra (along with the corresponding information and characteristics) and one can directly perform simulations using any evaluated cross-section dataset online, in order to validate the specific data and check their reliability before use.

Benchmarks of the **^{23}Na(p,p)** backscattering, using the NaBr pellet with a thin layer of gold on top, regarding the evaluated cross-section data, which range only up to 1500 keV, can be seen in Figures 5. At such low energies, the spectra are dominated by the signal of the heaviest element in the compound target, which is Br. Despite the resulting poor statistics (5% uncertainty in the worst case), originating from the subtraction of the large Rutherford Br signal from the total experimental one (over the whole integrated region corresponding to 250 keV from the surface), the simulation seems to reproduce the experimental spectra quite well for all the studied angles and the evaluated data are thus in principle validated.

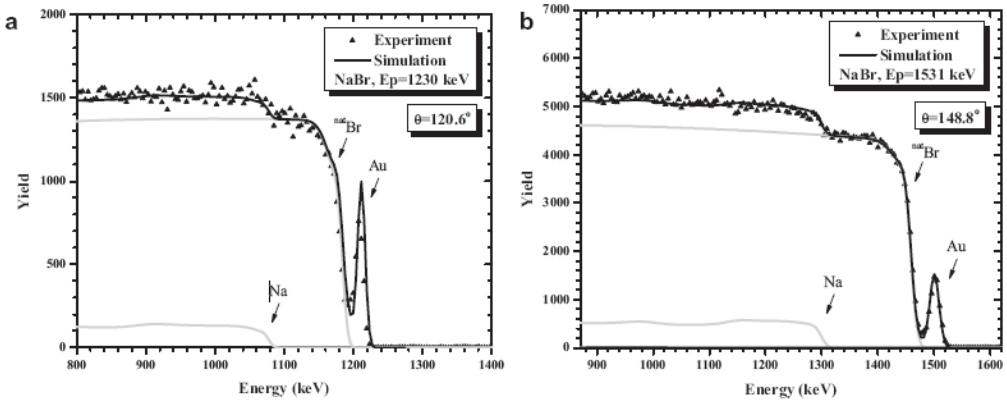

Figures 5. (a and b) Benchmarking results for ^{23}Na(p,p) using the corresponding evaluated cross-section datasets for the simulations at different beam energies and detection angles .

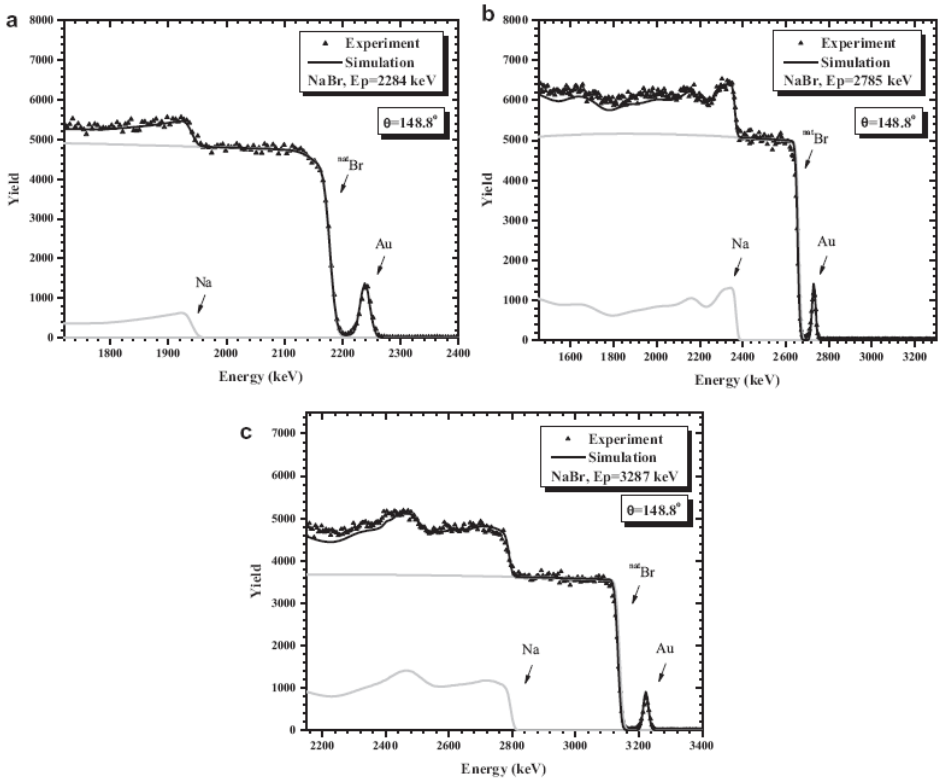

Figures 6. (a–c) Benchmarking results for ^{23}Na(p,p) at 150°, using the experimentally determined cross-section dataset by Caciolli et al. [19] for the simulations at different beam energies.

The benchmarking at higher energies was performed using the only available data of Caciolli *et al.*[19] at 150°, plotted in Figures 6. The simulations using these experimentally determined differential cross sections are in excellent agreement with the experimental spectra within the total experimental uncertainty (4%) except for the low energy case (at 2284 keV) where the agreement is within 7%. This dataset is thus validated and can be recommended for EBS analytical purposes. Moreover, it can be used for the extension of the evaluation to higher energies.

The evaluated cross sections for the **^{31}P(p,p)** backscattering exist up to 2000 keV [1] showing a rather complicated structure with narrow resonances. The results of the corresponding benchmarking using a GaP wafer with a thin layer of gold on top as target,

showed a very good agreement (within 3-4%, over a small energy window) between the simulations and the experimental thick target spectra in the energy range up to 1782 keV, as can be seen in Figures 7a-b. The evaluated data at higher energies needed to be tuned according to the present experimental work and the reproduction of the thick target spectra by the simulations using the revised evaluated cross sections (SigmaCalc 2.0) was found to be eventually excellent, as presented in Figure 7c. The actual comparison between the two versions of SigmaCalc is presented in Figure 7d.

At higher energies the only existing experimental dataset, related to the detection angles studied in the present work, is the one by Karadzhev *et al.* [20] up to 3500 keV for the ^{31}P(p,p) backscattering at 150°. The corresponding benchmarkings showed serious discrepancies between the simulated (using the data of [20]) and measured spectra (actually it seems that the data of Karadzhev *et al.* are systematically underestimated) as seen in Figures 8. This dataset cannot thus be recommended for analytical purposes, despite the fact that there seems to be a clear qualitative agreement. Consequently, it cannot be directly incorporated in the evaluation procedure at higher energies and therefore further experimental studies are needed in this case.

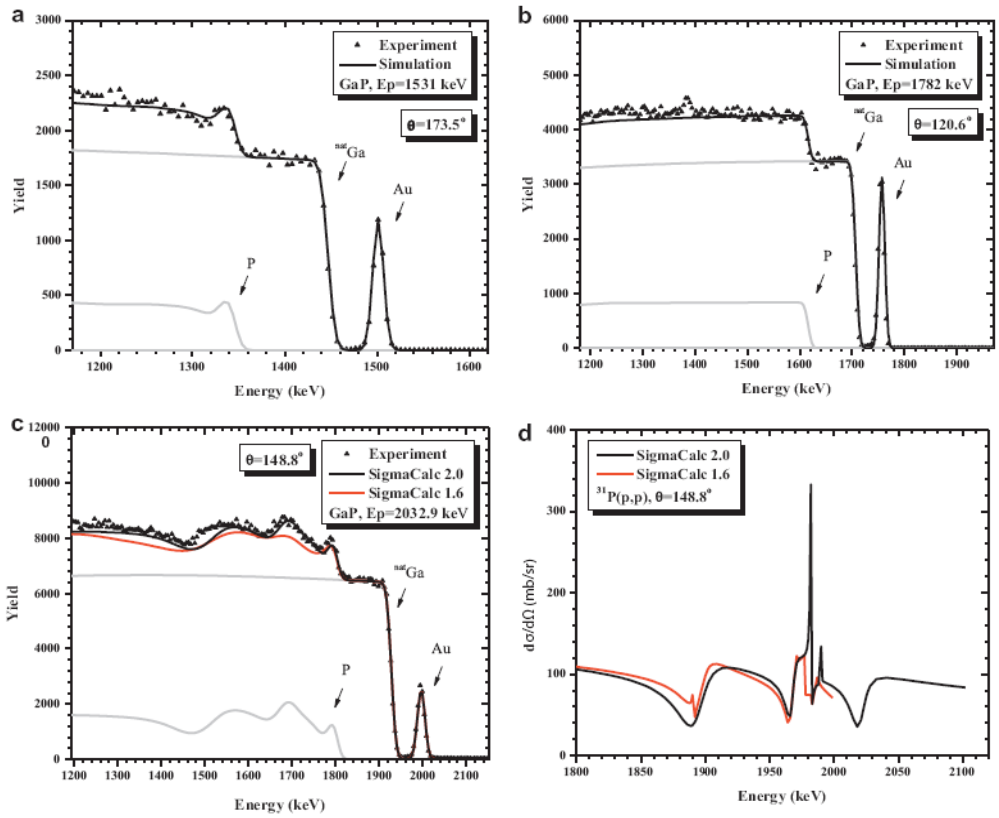

Figures 7. (a–c) Benchmarking results for ^{31}P(p,p) using the corresponding evaluated cross-section datasets for the simulations at different beam energies and detection angles. (d) Comparison between the two versions of SigmaCalc.

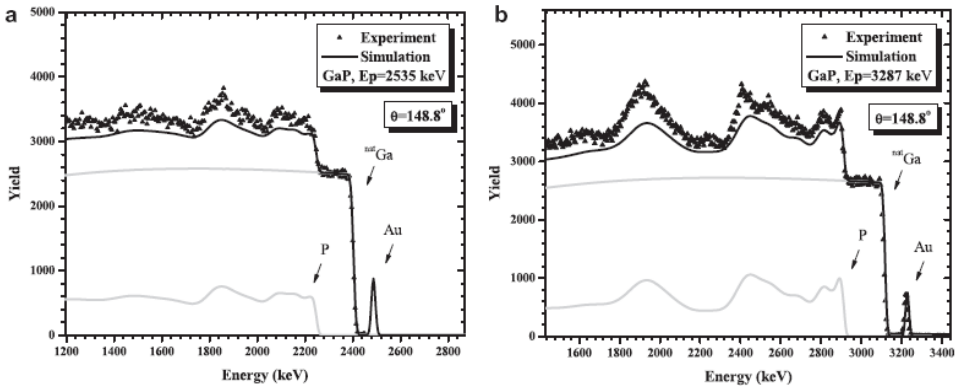

Figures 8. (a and b) Benchmarking results for ^{31}P(p,p) at 150°, using the experimentally determined cross-section dataset by Karadzhev et al. [20] for the simulations at different beam energies.

Proton backscattering on ^{nat}**B** was studied in the present work, both by using standard NIM electronics and by implementing the ΔE/E technique up to 3.3 MeV, due to the background contribution from alpha particles (originating from (p,α) reactions). With the use of a ΔE/E telescope, the detected protons and alphas are eventually separated, thus enabling two different ways to further analyze the data. The first one is to directly perform simulations of the protons acquired by implementing the telescope and the second one to study the acquired alphas instead. Each simulation of the protons acquired by implementing the telescope depended on the energy loss and straggling in the corresponding thin ΔE detector. In order to reproduce these effects in the simulated spectra, a proper silicon foil, namely of the same thickness of the corresponding thin detector, was used as absorber foil in all simulations. The nominal thickness of the ΔE detectors used was checked experimentally and was eventually determined using a triple alpha source with an accuracy of the order of 4%.

The study on the other hand of the detected alphas showed a linear dependence with energy, which enabled a linear regression rule to be applied. Thereby their contribution to the obtained yield when using standard NIM electronics could be subtracted. This way the simulation procedure and thereby the validation process is simplified, as it does not depend on any straggling function (other than the one in the studied material).

Both techniques present distinct inherent disadvantages. The former strongly depends on the accuracy of the straggling function and the thickness of the ΔE detector which acts as an absorber foil, while the latter ignores any possible variations in the underlying alpha background. Providing also that there still seem to be discrepancies between both implemented techniques for the same energy window, the complete analysis will be the subject of a complementary future study.

Conclusions

A benchmarking methodology has been developed and documented in the present work regarding the validation of charged particle differential cross sections, using thick target yields. This procedure has been implemented to validate the evaluated (and/or the existing experimental) cross-section datasets, concerning critical EBS data for IBA. In particular, the benchmarking measurements of the present work involved the validation of the existing differential cross sections of proton elastic scattering on ^{nat}S, ^{23}Na and ^{31}P up to 3.5 MeV. The corresponding studied evaluated data were found to be valid in most of the cases (in terms of energy regions and scattering angles), while selected benchmarks of experimentally determined cross sections (in the absence of evaluated ones at higher energies) indicated the reliable datasets, which could potentially be used in the corresponding evaluation process in order to extend it to higher energies. Moreover,

the benchmarking procedure in the complicated case of $^{nat}B(p,p)$, where a strong background contribution from alpha particles exists, has been investigated both by using standard NIM electronics and by implementing the ΔE/E technique up to 3.3 MeV and the analysis is still in progress.

Acknowledgements
This work has been supported by the European Community as an Integrating Activity 'Support of Public and Industrial Research Using Ion Beam Technology (SPIRIT)' under EC contract no. 227012.

References

[1] SigmaCalc: http://sigmacalc.iate.obninsk.ru, www-nds.iaea.org/exfor/ibandl.htm

[2] A.F. Gurbich, Evaluated differential cross-sections for IBA, Nucl. Instr. Meth. B 268 (2010) 1703.

[3] D. Abriola, A.F. Gurbich, M. Kokkoris, A. Lagoyannis, V. Paneta, Nucl. Instr. Meth. B 269 (18) (2011) 2011.

[4] I.B. Radovic, Z. Siketic, M. Jakšic, A.F. Gurbich, J. Appl. Phys. 104 (7) (2008). art. no. 074905.

[5] A.F. Gurbich, C. Jeynes, Nucl. Instr. Meth. B 265 (2) (2007) 447.

[6] M. Mayer, *SIMNRA, a Simulation Program for the Analysis of NRA, RBS and ERDA*, Proceedings of the 15th International Conference on the Application of Accelerators in Research and Industry, J. L. Duggan and I.L. Morgan (eds.), American Institute of Physics Conference Proceedings 475 (1999) 541.

[7] N.P. Barradas, C. Jeynes, Advanced physics and algorithms in the IBA DataFurnace, Nucl. Instrum. Meth. B 266 (8) (2008) 1338.

[8] J.F. Ziegler, J.P. Biersack, and U. Littmark. The Stopping and Ranges of Ions in Matter.
Pergamon Press, New York, 1985.

[9] W.K. Chu. Phys. Rev. 13 (1976) 2057.

[10] Q. Yang, D.J. O'Connor, and Z. Wang. Nucl. Instr. Meth. B 61 (1991) 149.

[11] INDC(NDS)-0634, Accuracy of Experimental and Theoretical Nuclear Cross-Section Data for Ion Beam Analysis and Benchmarking, Summary Report of the Consultants' Meeting, 2013.

[12] E.V. Gai, A.F. Gurbich, Evaluated $^{12}C(^{4}He,^{4}He)^{12}C$ cross-section and its uncertainty, Nucl. Instr. Meth. B 296 (2013) 87.

[13] C. Chronidou, K. Spyrou, S. Harissopulos, S. Kossionides, T. Paradellis, Eur. Phys. J. A 6 (1999) 303.

[14] J.B. Marion, Accelerator calibration energies, Rev. Mod. Phys. 38 (1966) 660.

[15] P. Rao, S. Kumar, S. Vikramkumar, V.S. Raju, Nucl. Instr. Meth. B 269 (2011) 2557;
P.M. Endt, Nucl. Phys. A 633 (1998) 1.

[16] S.L. Molodtsov, A.F. Gurbich, C. Jeynes, Accurate ion beam analysis in the presence of surface roughness, J. Phys. D: Appl. Phys. 41 (2008) 205303.

[17] CN/ASD Group. MINUIT, Users Guide, nProgram Library D506. CERN, 1993.

[18] H.H. Andersen, J.F. Ziegler, Hydrogen – Stopping Powers and Ranges in All Elements, Pergamon Press, New York, 1977.

[19] A. Caciolli, G. Calzolai, M. Chiari, A. Climent-Font, G. Garcia, F. Lucarelli, S. Nava, Proton elastic scattering and proton induced c-ray emission cross-sections on Na from 2 to 5 MeV, Nucl. Instrum. Meth. B 266 (8) (2008) 1392.

[20] K.V. Karadzhev et al., YadernayaFizika 7 (1968) 242. Available from: http://www-nds.iaea.org/exfor/ibandl.htm.